ATR Performance within an Extended X-Band Tower-Turntable Database of Highly Resolved Relocatable Targets

Timo Kempf, Markus Peichl, Stephan Dill, Helmut Süß
DLR (German Aerospace Center)
Microwave and Radar Institute
P.O.-Box 11 16,
82230 Wessling
Germany

ABSTRACT

By means of data from highly resolved tower-turntable ISAR measurements this paper investigates the ATR robustness of small changes in the articulation of targets (e.g. military vehicles) and changes in the incidence angle. The recognition process is based on a template matching method. The two-dimensional templates are generated by extracting the most robust scatterers from the RCS image.

1. INTRODUCTION

Global and reliable reconnaissance using remote sensing techniques requires weather and daytime independent detection, recognition, and identification of interesting objects. Thus a spaceborne high resolution synthetic aperture radar (SAR) system in a spotlight mode can be an appropriate instrument. On this basis we undertook X-band ISAR-measurements on a tower-turntable arrangement to get highly resolved two-dimensional signatures of military and civilian relocatable targets for adequately steep depression angles. Our work is focused on the military vehicles, and we use civilian vehicles as confusers.

Since typical military vehicles consist of several ideally behaving scattering centers which show some robustness to aspect variations, we established a recognition method based on the extraction of these point scatterers. Furthermore, with a demanded declaration time that is sufficiently long, we have the freedom to perform classification via a computationally intensive template matching process. Moreover this method ensures a sufficient inner class robustness, while simultaneously yielding efficient inter class separability.

This paper shall give an overview of the performance of the introduced ATR method using the tower-turntable database, which includes several thousand templates. The classifiers are evaluated by ROC-curves and confusion matrices. To examine the robustness of this recognition method we focus on different articulations of the targets. The articulations were realized by changing the position or pose of movable vehicle parts such as hatches, turrets, and assemblies, or by using camouflage. Additionally, we used small variations of the elevation angle or a modified ground. The results should also provide insight into how many different realizations and poses of one target type have to be stored in a database.

In [1] we already described an attempt to introduce a kind of fingerprint analysis as a situation-optimized tool for reliable target recognition.

The development and investigation of our method is based on ISAR measurements in X band carried out on military vehicles for different steep depression angles realized by a suitable tower-turntable arrangement as shown in fig. 1.

Paper presented at the RTO SET Symposium on "Target Identification and Recognition Using RF Systems", held in Oslo, Norway, 11-13 October 2004, and published in RTO-MP-SET-080.

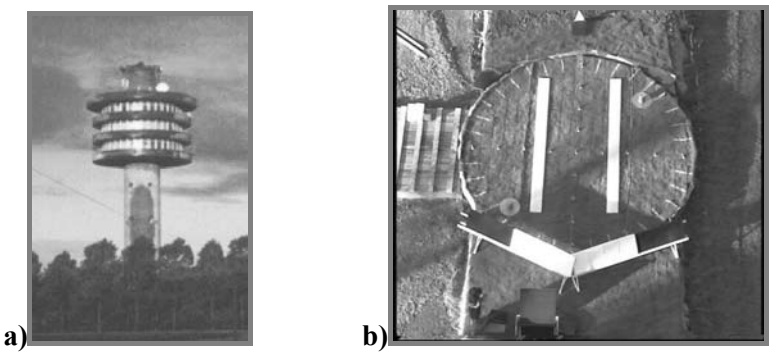

Figure 1: Tower-turntable setup for ISAR measurements, a) four platforms on the tower allow different incidence angles, b) the turntable was covered with soil and grass for a realistic ground, having 9m in diameter and a payload up to 100t.

These data have been used to develop a tomographical processing scheme that delivers a filtered and digitized radar image of those target scatteres, which behave strongly like ideal point scatterers and which are robust to aspect angle variations as illustrated in **fig. 2**.

In a practical use of a military reconnaissance operation such digitized images of an actual scene of interest can be compared successively to similarly processed image templates of a database. In principle, a type specific classifier correlates the current digitized test image with each training image, delivering the highest of the generated correlation values. In the following this value is also used as 'discrimination value'. Our first results indicated that this kind of fingerprint analysis can deliver reliable recognition results with a feasible amount of computational effort.

In order to assess the robustness of this recognition method many ISAR measurement campaigns have been undertaken in the past with focus on small variations of the targets or the scene. The results should also provide an idea how many different realizations of one target type have to be stored in a database, or which poses could be neglected, respectively.

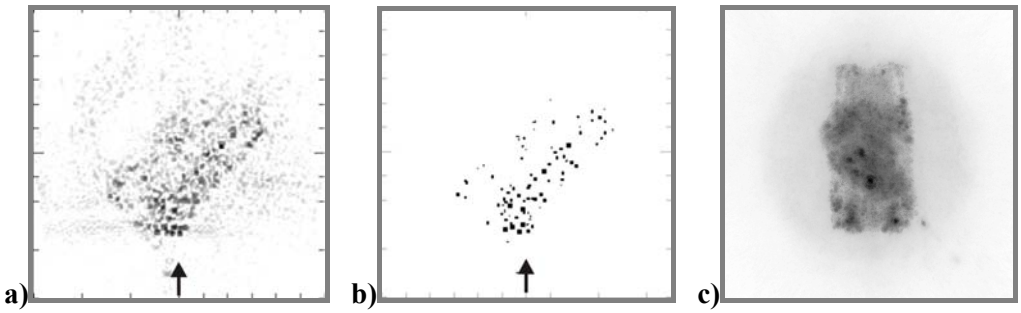

Figure 2: Example of a tomographically processed image, a) RCS after sidelobe suppression, b) a filtered version with the most reliable scatterers for use in ATR, c) an incoherent superposition of single images for a whole 360° rotation of the turntable. The turret and the gun were turned by 40° compared to the vehicles main axis.

The target list of our last campaign included military and civilian vehicles, whereas the intention of the ATR system design is focused on the military targets and the civilian vehicles are mainly used as confusers. Variants have been realized by changing the position or pose of movable vehicle parts like hatches, turrets, and assemblies, for instance, or by partially covering the targets with natural obstacles. Additionally small variations of the elevation angle or a modification of the ground have been used.

For the evaluation of the ATR results, the commonly used receiver operating characteristic (ROC) curves and confusion matrices are computed.

2. CLASSIFICATION RESULTS

The vehicles used are two **battle tanks** of different type (**BTa** and **BTb**), a **lorry** (**LOR**), a military **all-terrain vehicle** (**ATV**), a **VW bus** (**VWB**), a **tractor** (**TRA**), a **weapon-carrier** (**WCA**), and an optical **mockup** of the **weapon-carrier** (**MWC**).

2.1 Test data and training data with different polarization

Measurements were undertaken in HH polarization as well as in VV polarization. In order to demonstrate our approach applied to military targets the data set was divided into VV training data and HH test data. If the target provides enough "ideal" scattering centers like corners, we can expect a satisfying recognition performance. Each data set includes 72 templates corresponding to images in 5° azimuthal steps.

In detail the HH test data includes 12 data sets, 4 sets of battle tank 'a' as shown in **Fig. 3** by no. 1 to no. 4 along the horizontal axis, 4 sets of battle tank 'b' labeled by no. 5 to no. 8, 1 set of the lorry labeled by no. 9, 1 set of the all-terrain vehicle labeled by no. 10, and 2 sets of the VW bus labeled by no. 11 and no. 12. The VV training data includes the same targets with identical articulations and identical measurement geometry. Thus, for each test class a classifier could be established. It should be noted, that the SNR of the HH data was about 15dB less than that of the VV data due to technical reasons.

Fig. 3a) shows the discrimination behaviour of the BTa classifier (fed with the VV data set) for each test template from the 12 HH test data sets. A discrimination value d_{BTa}=1.0 would signify perfect identity of test and training template. **Fig. 3b)** shows the discrimination results of the BTb classifier, **fig. 3c)** that one of the LOR classifier, **fig. 3d)** that one of the ATV classifier, and **fig. 3e)** the discrimination results of the WCA classifier.

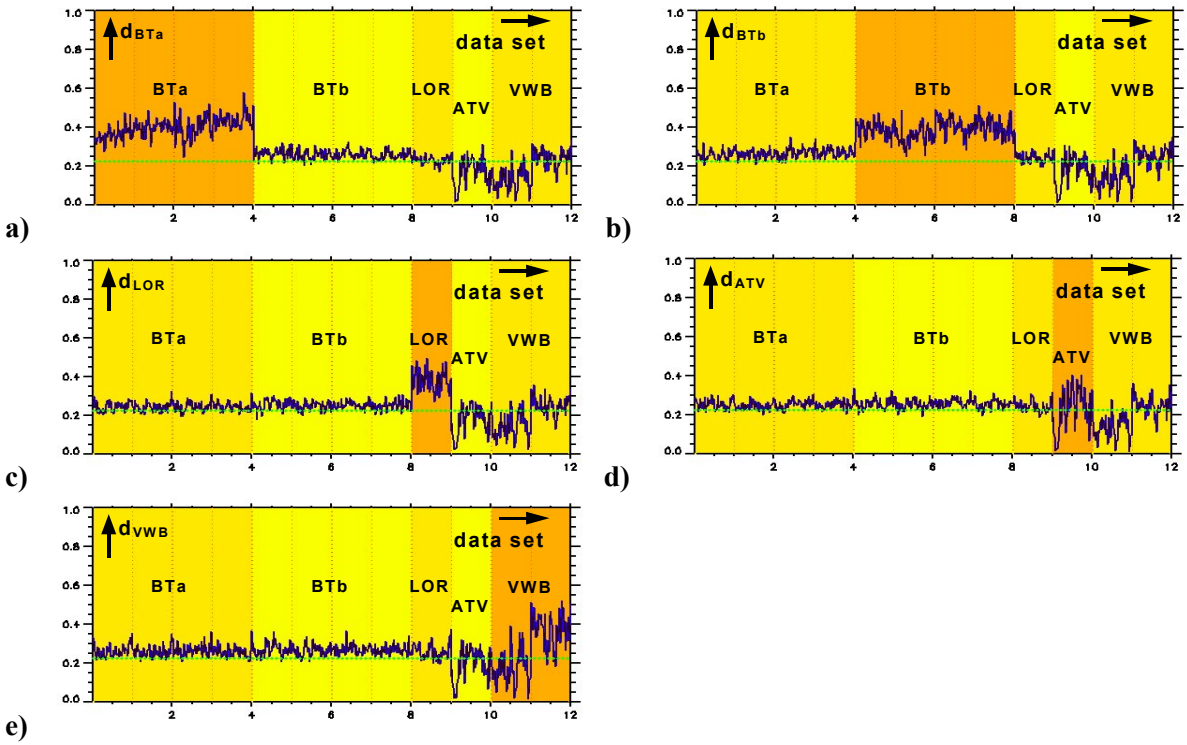

Figure 3: Discrimination results of the classifiers, for a description see text.

The dotted horizontal line represents the decision line for generating the confusion matrix as described below. The discrimination values of the classifiers for the battle tanks are well above this decision line and the discrimination values of the confuser vehicles.

A common tool to represent the property of a classifier is the ROC curve as shown in **fig. 4**. It relates the percentage of correct classification P_{CC} to the percentage of false alarms P_{FA}. This means, for a well adopted classifier the ROC curve will start at the point {1,1} in the graph, then move with a rising threshold close to the ideal point {0,1} corresponding to 100% of correct classification and no false alarm, and finally it drops down to the point {0,0} [2].

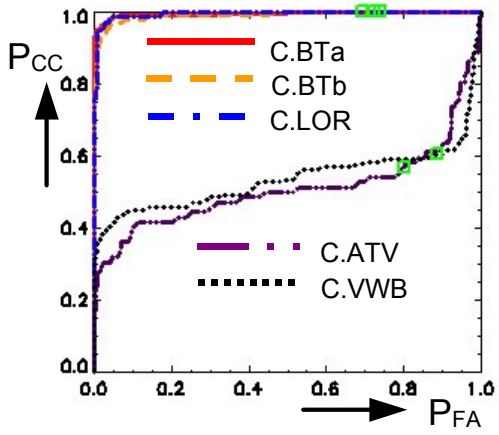

Figure 4 : ROC curves for the classifiers of fig. 3.

The squares mark the threshold points for the confusion matrix. The ROC curves for the battle tank classifiers are close to the ideal point. This confirms our assumption, that a method based on the highly resolved local distribution of robust scatterers applied to these types of vehicles would enable ATR. Additionaly the ROC curve of the lorry classifier shows the same performance, while the ROC curves of the ATV classifier and the VW bus classifier perform worse, since these targets deliver a far less number of robust scatterers.

Table 1a) below shows the corresponding confusion matrix, enabling the comparison of different classifiers on fixed values [3]. The rows represent the test data sets, and the columns denote the training data sets. The column 'OUT' includes the case, where the test target was not part of the training data, respectively. The numbers in the confusion matrix state how many templates of the current test data set yield a discrimination value in the classifier higher than a fixed threshold and higher than the values of the other classifiers. If no other classifier exceeds the threshold, the template is counted to the 'OUT' class.

As a common practice the threshold is chosen to a value that forces the classifiers to declare $P_D = 0.9$. Then the confusion matrix can be reduced to the percentage of correct classification as given by the numbers in the diagonal, and related to the number $P_{CC|D}$ of contributing templates for the fixed P_D. Here it is 98.46%. **Table 1b)** shows these percentages within the rows of the confusion matrix.

The results for the two battle tanks and the lorry show nearly ideal results, and the ATV and the VW bus show a high rejection rate. However, there is a low misclassification rate as indicated by the high $P_{CC|D}$ .In principle this indicates a high performance of this ATR method.

Table 1a). Confusion matrix for the VV trained classifiers on HH test data.

	C.BTa	C.BTb	C.LOR	C.ATV	C.VWB	*OUT*
BTa	**287**	1	0	0	0	***0***
BTb	0	**288**	0	0	0	***0***
LOR	0	0	**71**	0	1	***0***
ATV	2	0	0	**37**	4	***29***
VWB	1	1	1	1	**83**	***57***

Table 1b). Confusion matrix with normalized rows for the VV trained classifiers on HH test data.

	C.BTa	C.BTb	C.LOR	C.ATV	C.VWB	*OUT*
BTa	**99.7**	0.3	0	0	0	***0***
BTb	0.0	**100.0**	0.0	0.0	0.0	***0.0***
LOR	0.0	0.0	**98.6**	0.0	1.4	***0***
ATV	2.8	0.0	0.0	**51.4**	5.6	***40.3***
VWB	0.7	0.7	0.7	0.7	**57.6**	***39.6***

2.2 Test data and training data of different articulations or measurement geometry

The list in table 2a) gives an overview of the training data. The test data consist of the sets listed in table 2b), which almost all are given in VV-polarization*. This list describes first the target type, then the incidence angle, and finally some special articulations.

Table 2a). List of the training data (set number, type, incidence angle, polarization).

1. **BTa 45° HH + VV**
2. **BTb 50° HH + VV**
3. **LOR 50° VV**
4. **ATV 45° HH + VV**
5. **VWB 50° HH + VV**
6. **WCA 45° VV**

Table 2b). List of the test data (set number, type, incidence angle, special articulations).

1.	BTa	45°	no snow crosses
2.	BTa	45°	no snow crosses, hatches open
3.	BTa	45°	turret heading 20°
4.	BTa	45°	turret heading 40°
5.	BTa	42.5°	
6.	BTa	47.5°	
7.	BTa	50°	
8.	BTa	45°	turret heading 90°
9.	BTa	45°	turret heading 180°
10.	BTa	45°	metal plates on ground
11.	BTb	42.5°	
12.	BTb	45°	
13.	BTb	47.5°	
14.	BTb	50°	turret heading -45°
15.	BTb	50°	turret heading -90°
16.	BTb	50°	metal plates on ground
17.	BTb	50°	natural camouflage
18.	LOR	42.5°	
19.	LOR	45°	
20.	LOR	47.5°	
21.	ATV	47.5°	
22.	ATV	50°	
23.	VWB	47.5°	*(HH-polarization)
24.	VWB	47.5°	
25.	TRA	45°	
26.	WCA	42.5°	
27.	WCA	47.5°	
28.	WCA	50°	
29.	WCA	45°	natural camouflage
30.	MWC	45°	

Fig. 5 shows the discrimination results of the classifiers. The discrimination graphs show that the classifiers produce different results for different target articulations. Therefore a closer look on the corresponding ROC curves and confusion matrices shown in **fig. 6** is helpful. **Fig. 6a)** shows a perfect ROC curve for test data set no. 1 and no. 2 where the difference between the test and training data are mounted or dismounted snow crosses or closed or opened hatches. Even though these variations have stronger influences on the radar images as a whole, they offer quite enough redundancy for our ATR approach.

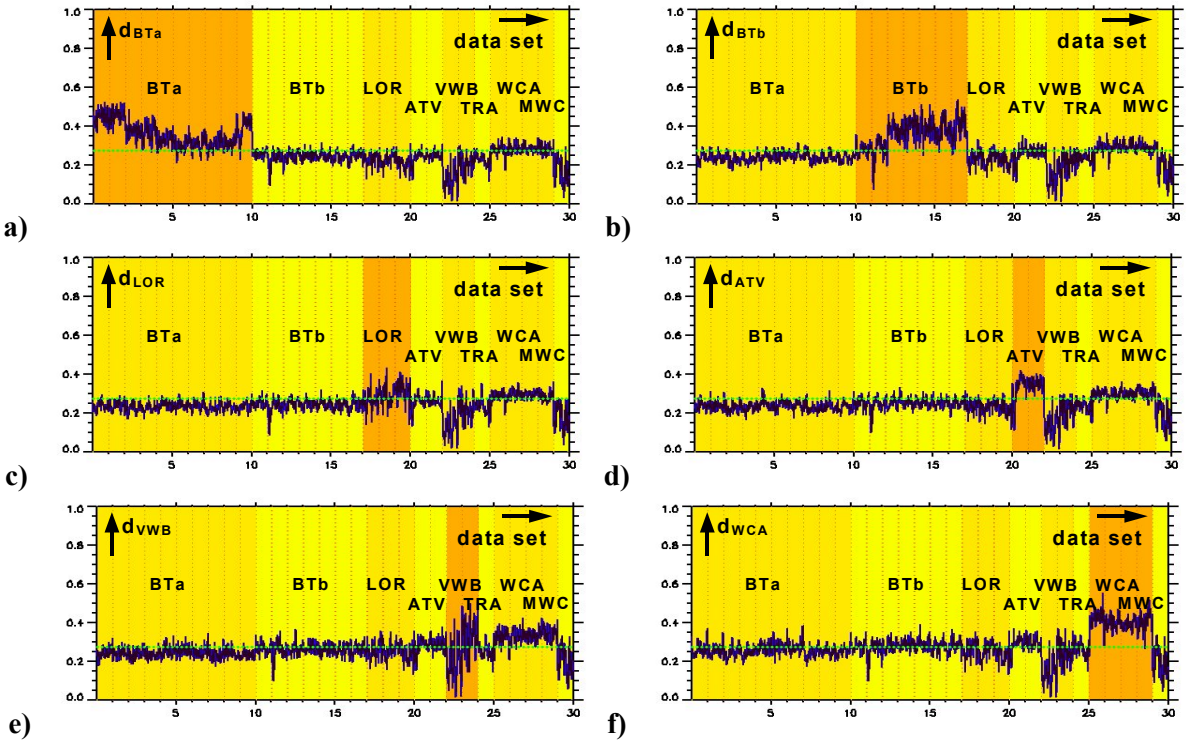

Figure 5: Discrimination results of the classifiers. a) BTa classifier, b) BTb classifier, c) LOR classifier, d) ATV classifier, e) VWB classifier, f) WCA classifier.

A stronger impact on the ATR performance is visible for the case of covering the natural grassy ground with metal plates, as it has been done in the test data sets no. 10 and no. 16 shown in **fig. 6a)** and **fig. 6b)**. The P_{CC} drops down to values below 0.9 and 0.8 for a P_{FA}=0 value.

Similar results can be observed for targets covered with natural camouflage as in the cases of test set no. 17 shown in **fig. 6b)** and no. 29 shown in **fig. 6j)**. Even though the radar images as a whole show serious differences, a satisfying recognition rate can be achieved. Here only the surface of the targets was covered, but much more information is given by the wheels and chassis structures at the sides of these vehicles.

In another test series the turret heading of the battle tanks was varied. **Fig. 6c)** and **6d)** show the corresponding ROC-curves with a very high and thus impressive robustness. This results again from the fact that the most important information is derived from the chassis. The highest degradation of the ATR performance can be observed for test set no. 8. Here the tank has a rather big turret covering a lot of the lower located scatterer centers in this position. The turret structure of the BTb is smaller, and so we don't see such a strong influence on the ROC curve for a similar heading in set no. 15.

Stronger impacts on the ATR performance are visible for differences in the incidence angle between training and test data, even for small variations. **Fig. 6e)** illustrates the results for a difference of 2.5° in incidence angle for the set no. 5 and no. 6, and 5° for set no. 7). **Fig. 6f)** shows the corresponding graphs for an incidence angle difference of 7.5°, 5° and 2.5° corresponding to nos. 11, 12, 13. In this case the 2.5° difference between training and test has less impact on the ROC-curve, but the 5° case gives worse results. In general it can be stated, that there is very much information available from the chassis parts of the tanks, which is relevant for our ATR approach. Due to the steep elevation angles as pretended by space-borne radars, the overlay effect in the SAR imaging can distort the relative location of the scatterers in the templates [4].

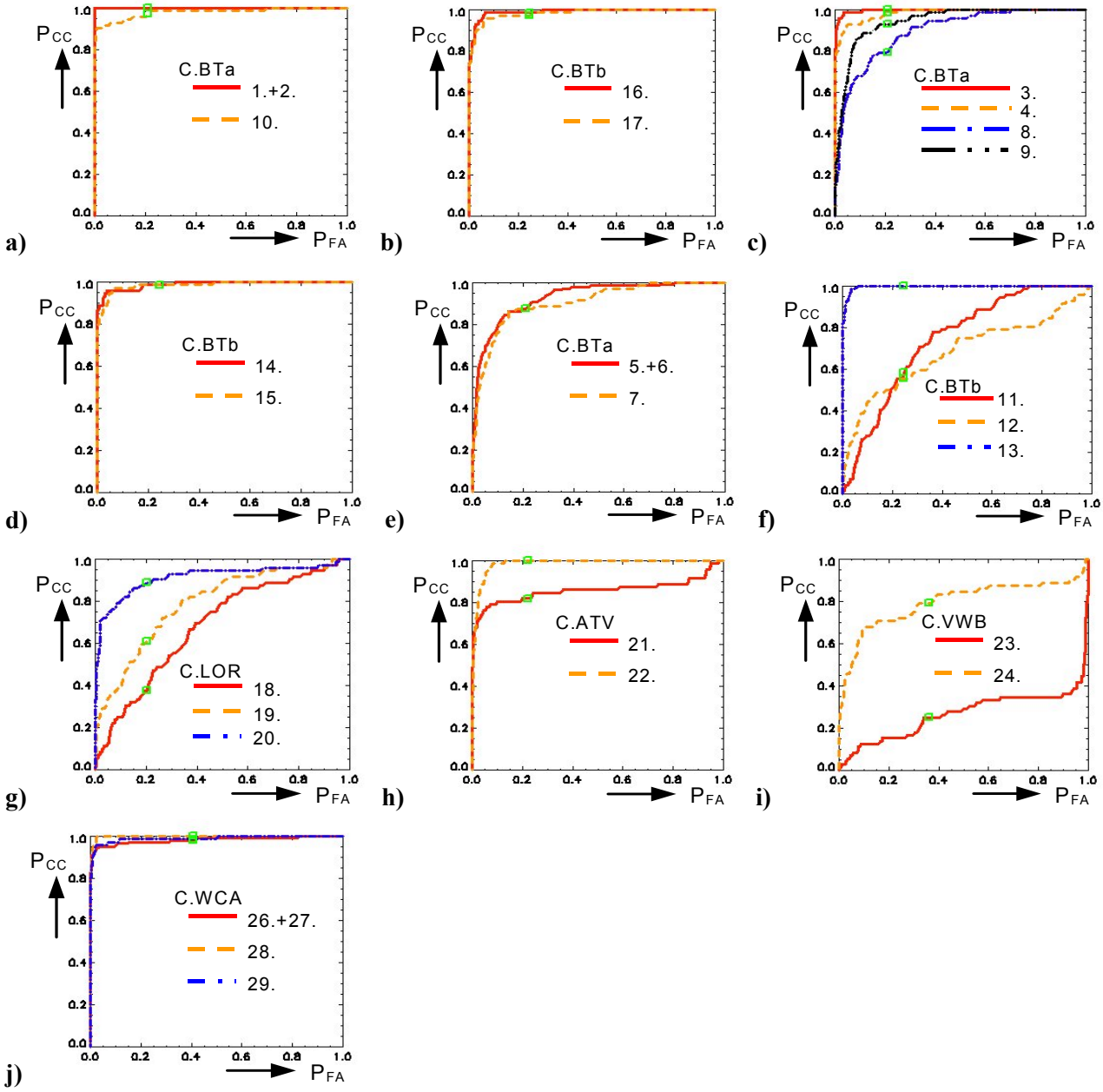

Figure 6: ROC curves for different classifiers and data sets of table 2. See text for further information.

The graph in **fig. 6g)** for the LOR confirms the above observed tendency. The reason that the results of the ATV in **fig. 6h)** don't fit into this behaviour was a SNR problem in the first part of data set no. 21. The worse SNR of the HH data also causes the wide spread of the ROC-curves in **fig. 6i)**, where identical geometrical conditions of the target have been used.

Some additional information about the classifiers may be extrcated from the confusion matrices listed in **table 3**. The P_D is again chosen to 0.9, but here without the confuser data sets of the TRA and the MWC. The corresponding $P_{CC|D}$ is 0.83. The mostly high numbers of the battle tank classifiers confirm the results of **fig. 6**. Note the very low number of misclassifications of the other battle tank, the other non-tank-like targets, and the confusers. However, this performance could easily be optimized by an adaption of the P_D value to the exclusive characteristics of the battle tank classifiers.

Table 3a). Confusion matrix for the data of table 2.

	C.BTa	C.BTb	C.LOR	C.ATV	C.VWB	C.WCA	*OUT*
BTa	**649**	2	1	1	11	23	***33***
1.+2.	**144**	0	0	0	0	0	***0***
3.	**72**	0	0	0	0	0	***0***
4.	**70**	0	0	0	0	1	***1***
5.+6.	**115**	0	0	0	4	16	***9***
7.	**59**	2	0	0	2	3	***6***
8.	**56**	0	1	0	1	3	***11***
9.	**64**	0	0	1	3	0	***4***
10.	**69**	0	0	0	1	0	***2***
BTb	5	**399**	1	0	17	39	***43***
11.	2	**21**	1	0	9	25	***14***
12.	3	**27**	0	0	7	9	***26***
13.	0	**72**	0	0	0	0	***0***
14.	0	**70**	0	0	0	2	***0***
15.	0	**69**	0	0	0	3	***0***
16.	0	**70**	0	0	1	0	***1***
17.	0	**70**	0	0	0	0	***2***
LOR	0	3	**113**	2	22	29	***47***
18.	0	1	**16**	2	14	13	***26***
19.	0	2	**36**	0	5	16	***13***
20.	0	0	**61**	0	3	0	***8***
ATV	0	0	1	**117**	6	11	***9***
21.	0	0	0	**53**	4	6	***9***
22.	0	0	1	**64**	2	5	***0***
VWB	0	0	0	1	**74**	0	***69***
23.	0	0	0	0	**18**	0	***54***
24.	0	0	0	1	**56**	0	***15***
WCA	0	1	0	0	15	**269**	***3***
26.+27.	0	0	0	0	5	**136**	***3***
28.	0	0	0	0	1	**71**	***0***
29.	0	0	0	0	9	**62**	***1***
TRA	0	2	2	2	9	19	***38***
MWC	0	0	1	1	6	9	***55***

Table 3b). Corresponding confusion matrix with normalized rows.

	C.BTa	C.BTb	C.LOR	C.ATV	C.VWB	C.WCA	*OUT*
BTa	**90.1**	0.3	0.1	0.1	1.5	3.2	***4.6***
1.+2.	**100.0**	0.0	0.0	0.0	0.0	0.0	***0.0***
3.	**100.0**	0.0	0.0	0.0	0.0	0.0	***0.0***
4.	**97.2**	0.0	0.0	0.0	0.0	1.4	***1.4***
5.+6.	**79.9**	0.0	0.0	0.0	2.8	11.1	***6.3***
7.	**81.9**	2.8	0.0	0.0	2.8	4.2	***8.3***
8.	**77.8**	0.0	1.4	0.0	1.4	4.2	***15.3***
9.	**88.9**	0.0	0.0	1.4	4.2	0.0	***5.6***
10.	**95.8**	0.0	0.0	0.0	1.4	0.0	***2.8***
BTb	1.0	**79.2**	0.2	0.0	3.4	7.7	***8.5***
11.	2.8	**29.2**	1.4	0.0	12.5	34.7	***19.4***
12.	4.2	**37.5**	0.0	0.0	9.7	12.5	***36.1***
13.	0.0	**100.0**	0.0	0.0	0.0	0.0	***0.0***
14.	0.0	**97.2**	0.0	0.0	0.0	2.8	***0.0***
15.	0.0	**95.8**	0.0	0.0	0.0	4.2	***0.0***
16.	0.0	**97.2**	0.0	0.0	1.4	0.0	***1.4***
17.	0.0	**97.2**	0.0	0.0	0.0	0.0	***2.8***
LOR	0.0	1.4	**52.3**	0.9	10.2	13.4	***21.8***
18.	0.0	1.4	**22.2**	2.8	19.4	18.1	***36.1***
19.	0.0	2.8	**50.0**	0.0	6.9	22.2	***18.1***
20.	0.0	0.0	**84.7**	0.0	4.2	0.0	***11.1***
ATV	0.0	0.0	0.7	**81.3**	4.2	7.6	***6.3***
21.	0.0	0.0	0.0	**73.6**	5.6	8.3	***12.5***
22.	0.0	0.0	1.4	**88.9**	2.8	6.9	***0.0***
VWB	0.0	0.0	0.0	0.7	**51.4**	0.0	***47.9***
23.	0.0	0.0	0.0	0.0	**25.0**	0.0	***75.0***
24.	0.0	0.0	0.0	1.4	**77.8**	0.0	***20.1***
WCA	0.0	0.4	0.0	0.0	5.2	**93.4**	***1.0***
26.+27.	0.0	0.0	0.0	0.0	3.5	**94.4**	***2.1***
28.	0.0	0.0	0.0	0.0	1.4	**98.6**	***0.0***
29.	0.0	0.0	0.0	0.0	12.5	**86.1**	***1.4***
TRA	0.0	2.8	2.8	2.8	12.5	26.4	***52.8***
MWC	0.0	0.0	1.4	1.4	8.3	12.5	***76.4***

In addition, **table 3** shows less performance for the WCA. The column of the WCA classifier shows several cases of misclassifications for other targets. This behaviour could be compensated by a scaling-down procedure for the discrimination values of the WCA classifier. However, we would not get the high performance of the battle tank classifiers as the WCA cannot deliver as much robust information due to its lower size.

Note that the confusion matrix shows a low number of misclassifications for the mock-up MWC by the WCA classifier, which could also be reduced by a corresponding raise of the decision threshold.

3. CONCLUSION

Based on data sets of ISAR tower-turntable measurements, this paper showed the high performance of our specific template matching method for the automatic recognition of battle tanks using a high resolution imaging radar. Special attention was given to the robustness of this method against small changes of the target articulation and pose. Even though the number of data for the special articulations was relatively small and the estimated statistics for the shape of the ROC curves and confusion matrices has therefore only a limited confidence, some concise tendencies could be observed.

In general, it can be recommended that for a training data base, regardless of using measured or synthetic data, more effort should be payed in different realisations of the sensor-target geometry like incidence and aspect angle than in many various articulations of the target. However, the application of our method on other targets than tanks has still to be evaluated.

4. REFERENCES

[1] Kempf, T., and M. Peichl, "A Method for Advanced Automatic Recognition of Relocatable Targets ", Proc. of RTO SET Panel, Prague, Czech Republic, Apr. 2002.

[2] R.A. English, "Classifier Evaluation Methodology using MSTAR Public Data Set", NATO working paper, DRDC Ottawa, Feb. 2003.

[3] Kempf, T., and M. Peichl, "Application of Complex Dual Apodization to high resolution low incidence angle ISAR images", Proc. of German Radar Symposium GRS, Berlin, Germany, Oct. 2000.

5. GLOSSARY

ATR	Automatic Target Recognition
ATV	All-Terrain Vehicle
BTa,BTb	Battle Tank type a/b
C.(BTa)	(Battle Tank type a)-Classifier
HH	Horizontal transmit/receive polarization
ISAR	Inverse SAR
LOR	Lorry
MWC	Mock-up of the Weapon Carrier
P_{CC}	Percentage of Correct Classification
$P_{CC\|D}$	P_{CC} for a fix P_D
P_D	Percentage of Declaration
ROC	Receiver Operating Characteristic
SAR	Synthetic Aperture Radar
SNR	Signal to Noise ratio
TRA	Tractor
VV	Vertical transmit/receive polarisation
VWB	Volkswagen Bus
WCA	Weapon Carrier